UNIVERSITY OF WISCONSIN

CENTER FOR PLASMA THEORY AND COMPUTATION

REPORT

Double-Helix Stellarator

P. E. Moroz

Center for Plasma Theory and Computation
Department of Engineering Physics
University of Wisconsin, Madison, Wisconsin 53706-1687

September 1997

UW-CPTC 97-16

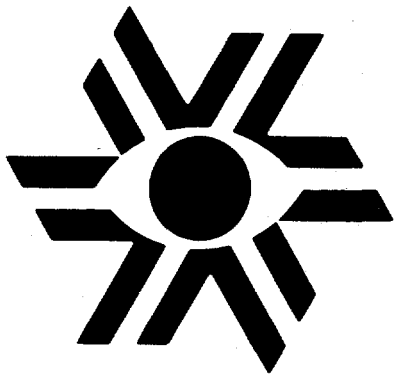

MADISON, WISCONSIN 53706-1687

DOUBLE-HELIX STELLARATOR

by

P. E. Moroz

Center for Plasma Theory and Computation

Department of Engineering Physics

University of Wisconsin, Madison, WI 53706, USA

September 1997

UW-CPTC 97-16

DOUBLE-HELIX STELLARATOR

Paul E. Moroz

Center for Plasma Theory and Computation
Department of Engineering Physics
University of Wisconsin, Madison, WI 53706, USA

Abstract.

A new stellarator configuration, the Double-Helix Stellarator (DHS), is introduced. This novel configuration features a double-helix center post as the only helical element of the stellarator coil system. The DHS configuration has many unique characteristics. One of them is the extreme low plasma aspect ratio, $A \approx 1 - 1.2$. Other advantages include a high enclosed volume, appreciable rotational transform, and a possibility of extreme-high-β MHD equilibria. Moreover, the DHS features improved transport characteristics caused by the absence of the magnetic field ripple on the outboard of the torus. Compactness, simplicity and modularity of the coil system add to the DHS advantages for fusion applications.

Introduction.

Low aspect ratio stellarators represent a fairly new area of research which was not paid much attention until very recently, and the lowest aspect ratio stellarators ever built have the aspect ratio, A (which is the ratio of the average major radius, R, to the average minor radius, a, for the last closed flux surface), of about A = 5. At the same time, lower aspect ratio and a stronger magnetic field (which is also much easy and less expensive to reach at low aspect ratios) are the main factors in advancing to controlled fusion, as can be explicitly seen from the well known LHD (Large Helical Device) scaling law [1] for the triple product, $nT\tau_E$, accessible in a stellarator,

$$nT\tau_E = 0.045\, a^{0.6} R^{-0.2} B^{2.4} P^{0.54} , \qquad (1)$$

where n is the average plasma density in 10^{19} m^{-3}, T is the average plasma temperature in keV, τ_E is the energy confinement time, in seconds, a and R are in meters, magnetic field strength, B, is in Teslas, and input power, P, is in MWatts.

The research program on very low aspect ratio stellarators, $A \leq 3.5$, called spherical stellarators (SS) in analogy with the spherical tokamaks (ST), has been proposed in [2], where the particular configuration with a straight center post has been considered and the advantages of a low aspect ratio for stellarators have been discussed. Very recently, a few other publications [3-16] have appeared on the topic of low aspect ratio stellarators.

How low can the plasma aspect ratio in a stellarator be? As it was mentioned in [2], in principle, very low-aspect-ratio stellarator configurations can be obtained simply by reducing the number of TF coils in a SS configuration. However, this way usually brings disadvantages of very low rotational transform, very strong outboard magnetic ripple, and very low equilibrium β limits.

In a recent publication [16], a new approach has been taken to reduce the aspect ratio in a stellarator further, a new class of stellarators has been introduced, the Extreme-Low-Aspect-Ratio Stellarators (ELARS), and a novel configuration, a Helical Post Stellarator (HPS), with $A \approx 1$, a single toroidal period, vacuum rotational transform $\iota \approx 0.1$ - 0.15, and advanced confinement characteristics, has been considered.

The present paper can be viewed as a continuation of research of Ref. 16 on ELARS configurations, which can be defined roughly as devices with stellarator features and $A < 1.4$. Here we consider a different ELARS device, the Double-Helix Stellarator (DHS), having the plasma aspect ratios of $A \approx 1$ - 1.2, two toroidal periods, and featuring a number of advanced characteristics. The purpose of the present paper is to introduce this novel configuration and give an initial demonstration of its advanced characteristics. While an analysis of Ref. 16 was limited to a vacuum magnetic field configuration, here we present results also for the finite plasma pressure and finite plasma current regimes, which demonstrate clearly significant advantages of ELARS for controlled fusion.

The rest of the paper is organized as follows. In Section II, the coil system of a DHS is presented and the main characteristics of the vacuum magnetic field are described. The results of calculations for the finite plasma pressure currentless regimes are presented in Section III. Positive effects of the plasma current are discussed in Section IV, and the advanced neoclassical transport characteristics of a DHS are described in Section V. Finally, the main conclusions are presented in Section VI.

II. Vacuum magnetic configuration of DHS.

The DHS coil configuration can be obtained from a typical ST coil system by replacing the straight center post of an ST with a double helix post, as shown in Fig. 1. The outboard parts of toroidal field (TF) coils can be the same as in an ST and, in principle, can even be replaced by a solid conducting wall to reduce the outboard magnetic field ripple.

The configuration presented in Fig. 1 corresponds to the first round of the coil system optimization regarding the extreme low aspect ratio, large enclosed volume, large vacuum rotational transform, small outboard magnetic field ripple, and small magnetic island structure. The coil system shown includes 24 outboard (half-elliptical) TF coils, 3 pairs of poloidal field (PF) rings, and a center post consisting of double-helix windings making 0.5 turns around the vertical axis.

In principle, the system of closed vacuum flux surfaces can be obtained even without PF rings. The vacuum magnetic field configuration described below

in this section corresponds to this case without the PF rings. However, the PF rings are very useful for controlling the equilibrium of high β plasmas (β is the ratio of plasma pressure to the magnetic field pressure), and thus will be used in the following sections.

The main reason why we chose a relatively large number (24) of outboard TF coils is because we would like to demonstrate that the outboard magnetic ripple can be practically fully suppressed in the ELARS considered. This situation is very similar to that in a tokamak, where the outboard magnetic ripple substantially reduces while increasing of the number of TF coils. For a demonstration of this effect, the $|B|$ variation along the field line for the last closed vacuum flux surface is shown in Fig. 2. This case corresponds to the current I_h = 600 kA flowing through each of the two helical elements of the center post and then returning through the outboard parts of TF coils. The last flux surface is chosen because it has the largest magnetic ripple. One can see clearly that the magnetic ripple is located practically entirely on the inboard of the torus. Later we will return to this question as it is important for good particle confinement in the device.

The perspective view of the last closed vacuum flux surface and the coils of the ELARS considered is shown in Fig. 3, which demonstrates a significant volume which the plasma can fill within the closed flux surfaces. The top view on the plasma is shown in Fig. 4. The configuration presented has the aspect ratio of about A = 1.2 and all helical disturbances of the magnetic field and toroidal asymmetries of the configuration are located on the inside of the torus.

The puncture plots for a set of closed vacuum flux surfaces obtained by following along the magnetic field lines are presented in Fig. 5 where the main cross-sections at toroidal angles $\varphi = 0, \pi/4$, and $\pi/2$ are shown. A large number of flux surfaces in Fig. 5 is chosen to demonstrate absence of magnetic islands or stochastic regions within the plasma.

To demonstrate the $|B|$ distribution on flux surfaces, Fig. 6 shows the distribution of $|B|$ over the last closed flux surface. There, B_0 represents the level corresponding to the first solid line, and ΔB is the difference between adjacent contours. The contours with values equal or above B_0 are shown by solid lines while those below B_0 - by the dash lines. This figure clearly demonstrates the peculiarity of the DHS configuration where the quasi-helical symmetry of $|B|$ is maintained in the inboard halves of flux surfaces while the quasi-toroidal symmetry is typical for the outboard halves. This is exactly opposite of a SS configuration of Ref. 2.

The vacuum rotational transform in this particular DHS is not very high. It varies from $\iota(0) = 0.095$ to $\iota(1) = 0.063$ as shown in Fig. 7, where $\iota = 1/q$, q being the safety factor. From the point of view traditional large-A stellarators, these values of ι are very small. However, one has to compare not the ι values themselves but rather the ι/A values having the meaning of the ratio of the average minor plasma radius to the connection length. These values are not smaller for this DHS than for traditional or advanced stellarators such, for example, as Wendelstein VII-X (W7-X) [17]. The typical descending character of radial dependence of ι makes the DHS to be similar to a tokamak. Addition of the plasma current in a DHS configuration will be thus natural and somewhat analogous to increasing of the plasma current in a tokamak.

In this paper, we did not try to thorough optimize the DHS system, which thus remains a large potential of further optimization. Nevertheless, the DHS configuration considered clearly demonstrates a number of significant advantages and a general potential of this ELARS approach for controlled fusion.

III. Finite pressure MHD equilibria in DHS.

Vacuum magnetic field configuration of a stellarator corresponds only to a relatively low plasma pressure. For a small experiment, where β cannot be large, this approach is adequate. However, from the point of view a large machine or, especially, a fusion reactor, the ability of a configuration to confine the high-β plasmas represents a significant advantage. Internal plasma currents, which may be high at high β, can modify the magnetic configuration significantly. The most important MHD equilibrium effects which might impose limitations on accessible β are the following: the Shafranov shift of the magnetic axis outboard, change of the plasma boundary shape, change of the rotational transform, and appearance or growth of the magnetic islands.

In the calculations presented in this paper, we are using the three-dimensional MHD equilibrium code, VMEC [18], running in the free-boundary mode. This code takes into account the actual conductors with the currents. All the above mentioned effects, except the magnetic islands can be thus addressed via this code.

There are no reasons to present here the MHD equilibrium cases with low β, as VMEC give the results which are close to those of the vacuum configuration, presented in Section II. More important is to demonstrate the possibility of high-β equilibria. One such case corresponding to the currentless MHD equilibrium with the central β_0 of 11% and the volume average β of 4.5% is presented below. These values of β are fairly high and, for comparison, are close to the predicted β limit [17] in the advanced stellarator W7-X.

The main cross-sections, $\varphi = 0, \pi/4, \pi/2$, of flux surfaces are presented in Fig. 8, while the radial profiles of the rotational transform, ι, magnetic well, W, and β values for this equilibrium are shown in Fig. 9. The radial variable, s, is the normalized enclosed toroidal flux. As usually, W is defined through the integral, $U = \int dl/B$, taken along a field line and averaged over the flux surface: $W(\rho) = 1 - \langle U(\rho) \rangle \; / \; \langle U(0) \rangle$.

As one can see, the main high-β effects are the following: (1) notable Shafranov shift of the magnetic axis outboard; (2) decrease of ι in the center and its increase at the edge, so the radial profile of ι changes to that of a typical large-A stellarator where ι increases with the minor radius; (3) appearing of a significant magnetic well, $W \approx 45\%$ in this case, which is normally of importance for good plasma stability characteristics; (4) change of the plasma shape; and (5) decrease of the plasma aspect ratio, which becomes $A \approx 1.05$.

The PF rings, which have not been used in the vacuum case, are of importance now, and carry the following currents: $I_{pf1} = 54$ kA (for the rings at R = 1.05 m), $I_{pf2} = 13.5$ kA (at R = 0.75 m), and $I_{pf3} = 160$ kA (at R = 0.3 m).

IV. Positive effects of plasma current.

According to the traditional stellarator approach (see, for example, [17, 19, 20]), a plasma current in a stellarator should be avoided. This includes not only the ohmically driven current but the bootstrap current as well.

In contrast, very positive effects of the plasma current have been identified [4, 5] for the SS configurations, where the ohmically driven current or bootstrap current produce such positive effects as an increase of the rotational transform and significant increase of the β limits.

Here we demonstrate that the plasma current is similarly advantageous for the DHS configurations. Addition of the positive plasma current (such current that the total rotational transform increases) has the effect of partially restoring the properties of vacuum flux surfaces in spite of the high plasma pressure: the Shafranov shift decreases and the plasma shape becomes closer to the vacuum one. These effects make possible further increase of the plasma pressure (correspondingly, the currents in the PF rings should be increased as well). An example of extreme-high-β MHD equilibrium ($\beta_o \approx$ 70%, $\beta \approx$ 30%) for this DHS with the plasma current of I_p = 160 kA is presented in Fig. 10. The plasma current profile is hollow, which models approximately what will happen with a bootstrap current. The limiting β values for a DHS considered are probably even higher than that just mentioned. The value of the plasma current used in this example is very moderate, and the total rotational transform is below $\iota = 0.5$ everywhere in the plasma. The radial profiles of β, W, ι, and the plasma current density, J, for the equilibrium of Fig. 10, are given in Fig. 11.

V. Advanced low-collisional transport characteristics of DHS.

The magnetic field characteristics of stellarators are normally substantially three-dimensional. Two known exceptions are represented by the so-called quasi-helically symmetric stellarators [21-24], when the magnetic field structure in Boozer coordinates [25-26] is close to the helically symmetric one, and the quasi-toroidally symmetric stellarators [13, 27, 28]. These two types of stellarators feature rather good neoclassical transport characteristics. However, they usually feature also a number of difficulties which prevent their possible projection to reactor parameters. One difficulty is related to the bootstrap current which normally appears in stellarators at high β. In so far found quasi-symmetric configurations, the bootstrap current is negative, which decreases the vacuum rotational transform and degrades the characteristics of a configuration. Another difficulty is related to the rather low β limits found so far for these configurations. Requirement on minimization of the bootstrap current and improvement of the high-β characteristics led the W7-X team [17, 29] to design of a stellarator system which is different from the quasi-symmetric one. In addition, the quasi-helical symmetry is not accessible in low aspect ratio devices and, thus, is not relevant to the chosen topic of ELARS.

Quasi-symmetry is advantageous for neoclassical transport. However, it is not a necessary requirement for improved transport characteristics of a stellarator. Another approach is to find a configuration without symmetry but with improved transport due to the so-called omnigenous particle drifts (i.e. having guiding-center orbits lying within the same flux surfaces) [30-32]. A set of criteria which can be used for the configuration optimization has been also

discussed in [33-34]. Here, we follow the recommendations [31, 32] to have the magnetic field ripple moved from the outboard to inboard parts of flux surfaces. The considered DHS configuration represents a clear example of this approach. Because of that, a DHS is characterized by an improved neoclassical transport.

Without carrying out time-consuming particle transport calculations, one can estimate the improvement in the low-collisional neoclassical transport from the S-factor [32] which for the general magnetic field of the form,

$$B / B_o = \sum_{mn} \varepsilon_{mn} \cos(m\theta - nN\varphi) , \qquad (2)$$

can be written as

$$S = \frac{1}{\rho^2} \int_0^{2\pi} d\theta \, \varepsilon_H^{3/2} \left[1.778 \left(\frac{\partial \varepsilon_T}{\partial \theta}\right)^2 - 2.133 \left(\frac{\partial \varepsilon_T}{\partial \theta}\right)\left(\frac{\partial \varepsilon_H}{\partial \theta}\right) + 0.684 \left(\frac{\partial \varepsilon_H}{\partial \theta}\right)^2 \right] , \qquad (3)$$

where

$$\varepsilon_T = \sum_{m \neq 0} \varepsilon_{m0} \cos(m\theta) \qquad (4)$$

$$\varepsilon_H = \sqrt{\left(\sum_m \varepsilon_{mn_0} \cos(m\theta)\right)^2 + \left(\sum_m \varepsilon_{mn_0} \sin(m\theta)\right)^2} \qquad (5)$$

To judge how good the configuration is optimized for the transport, it is useful to compare the S-factor given by Eq. (2) with the factor S_o calculated for the same configuration but including only the first term in the square brackets (so,

the cancellation caused by the terms with different signs, or enhancement, in the unfavorable case, cannot be realized):

$$S_0 = \frac{1.778}{\rho^2} \int_0^{2\pi} d\theta \, \varepsilon_H^{3/2} \left(\frac{\partial \varepsilon_T}{\partial \theta} \right)^2 \qquad (6)$$

The θ and φ angles in the above expressions correspond to the Boozer coordinate system [25-26].

Usually, for the low aspect ratio stellarators, which have the magnetic field ripple localized mostly outboard, the parameter, $S/S_0 >> 1$. For all DHS configurations considered in this paper, this ratio, S/S_0 , is lower than 1, and thus the low-collisional neoclassical transport is improved. For demonstration, Fig. 12 shows the radial dependence of S/S_0 for all three equilibria considered: for the vacuum case of $\beta = 0$ (solid curve), for the high-β currentless case (dashed curve), and for the extreme-high-β equilibrium with the plasma current (dotted curve).

VI. Discussion and conclusions.

A novel stellarator configuration, the Double-Helix Stellarator (DHS), is presented. This configuration has a number of features which are very unique and very unusual in comparison with those of presently known stellarators. This is an extreme-low-aspect-ratio stellarator (ELARS) system. It features extreme-low plasma aspect ratios, $A \approx 1$ - 1.2, not known before for stellarators. The DHS is a relative of a HPS configuration recently considered in Ref. 16. The

only helical elements of a DHS are the two helical windings replacing the center post of a standard spherical tokamak coil system. Actually, the DHS is featuring one of the most compact and the most spherical plasma among all SS configurations [2-12], and thus can be considered as a new member of the spherical stellarator family, as well.

In principle, the low aspect ratio stellarators are very advantageous for controlled fusion, as shown by the standard scaling laws [1]. The possible usual difficulty of the low-aspect-ratio stellarators, the unfavorable low-collisional neoclassical transport, can be overcome in the DHS due to the localization of the magnetic field ripple entirely on the inboard of the torus. Theoretically, it was shown [31-32] that such type of harmonic composition is the most efficient for collisionless plasma confinement. Our calculations of the S-factor [32] for different regimes in the DHS confirmed this conclusion.

The PF rings are not needed, in principle, for the vacuum stellarator configuration to exist. However, they are important at high β (and have been used in our calculations) for plasma control.

Analysis of the finite-plasma-pressure currentless regimes in the DHS demonstrated the possibility of high-β MHD equilibria ($\beta = 4.5\%$, $\beta_0 = 11\%$) which also feature the good particle transport characteristics.

In contrast to the usual opinion that a plasma current should be avoided in stellarators, our analysis demonstrates a number of advantages of having a plasma current in a DHS. This is analogous to the positive effects of the plasma current found for the spherical stellarator configurations [4, 5]. A

possibility of extreme-high-β ($\beta \approx 30\%$, $\beta_0 \approx 70\%$) MHD equilibria even with the moderate plasma current (such that the total rotational transform is below 0.5 everywhere in the plasma) has been demonstrated.

There is a significant potential (which we have just started to explore) of the DHS approach for controlled fusion, and further optimization of the DHS coil system will likely result in finding even higher β regimes with more advanced transport characteristics.

In conclusion, the author would like to thank S. P. Hirshman for permission to use the MHD equilibrium code, VMEC. This work was supported by the U.S. DOE Grant No. DE-FG02-97ER54395.

References.

[1] S. Sudo, Y. Takeiri, H. Zushi, F. Sano, K. Itoh, K. Kondo, A. Iiyoshi, Nucl. Fusion **30** (1990) 11.

[2] P. E. Moroz, Phys. Rev. Lett. 77 (1996) 651.

[3] P. E. Moroz, 23rd IEEE Conf. on Plasma Science, Boston, MA (Institute of Electrical and Electronics Engineers, 1996) p. 190.

[4] P. E. Moroz, Physics of Plasmas **3** (1996) 3055.

[5] P. E. Moroz, D. B. Batchelor, B. A. Carreras, S. P. Hirshman, V. E. Lynch, D. A. Spong, J. S. Tolliver, A. Ware, Fusion Technology **30** (1996) 1347.

[6] P. E. Moroz, Stellarator News **48** (1996) 2.

[7] P. E. Moroz, D. B. Batchelor, B. A. Carreras, S. P. Hirshman et al., Bull. Amer. Phys. Soc. **41** (1996) 1567.

[8] D. B. Batchelor, B. A. Carreras, S. P. Hirshman, V. E. Lynch, D. A. Spong, A. Ware, J. C. Whitson, Bull. Amer. Phys. Soc. **41** (1996) 1568.

[9] D. W. Ross, P. M. Valanju, H. He et al., Plasma Phys. Reports **23** (1997) 492.

[10] D. A. Spong, S. P. Hirshman, J. C. Whitson, Plasma Physics Reports **23** (1997) 483.

[11] P. E. Moroz, Plasma Physics Reports **23** (1997) 502.

[12] P. E. Moroz, "Low aspect ratio stellarators with planar coils", to appear in Plasma Phys. and Contr. Fusion (1997).

[13] P. R. Garabedian, Phys. Plasmas **4** (1997) 1617 .

[14] D. A. Spong, S. P. Hirshman, J. C. Whitson, Stellarator News **52** (1997) 1.

[15] P. E. Moroz, Nucl. Fusion **37** (1997).1045.

[16] P. E. Moroz, "Helical post stellarator", UW-Madison Report CPTC 97-15 (1997), submitted for publication.

[17] G. Grieger, W. Lotz, P. Merkel, J. Nuhrenberg, J. Sapper, E. Strumberger, H. Wobig etc., Phys. Fluids **B4** (1992) 2081.

[18] S. P. Hirshman, W. I. Rij, P. Merkel, Comp. Phys. Comm. **43** (1986) 143.

[19] H. Maassberg, W. Lotz, J. Nuhrenberg, Phys. Fluids **B5** (1993) 3728.

[20] P. R. Garabedian, H. J. Gardner, Phys. Plasmas **2** (1995) 2020.

[21] J. Nuhrenberg, R. Zille, Phys. Lett., **129A** (1988) 113.

[22] D. A. Garren, A. H. Boozer, Phys. Fluids **B3** (1991) 2822.

[23] D. T. Anderson, A. F. Almagri, F. S. B. Anderson, P. G. Matthews, J. L. Shohet, J. N. Talmadge, Bull. Am. Phys. Soc. **39** (1994) 1601.

[24] A. H. Boozer, Plasma Phys. Contr. Fusion **37** (1995) A103.

[25] A. H. Boozer, Phys. Fluids **25** (1982) 520.

[26] G. Kuo-Petravic, A. H. Boozer, J. A. Rome, R. H. Fowler, J. Comp. Physics **51** (1983) 261.

[27] J. Nuhrenberg, W. Lotz, S. Gori, "Quasi-axisymmetric tokamaks", in Theory of Fusion Plasmas, Societa Italiana di Fisica, Bologna 1994, p. 3.

[28] P. R. Garabedian, Phys. Plasmas **3** (1996) 2483.

[29] C. Beidler et al., Fusion Technology **17** (1990) 148.

[30] L. S. Hall, B. McNamara, Phys. Fluids **18** (1975) 552.

[31] H. E. Mynick, T. K. Chu, A. H. Boozer, Phys. Rev. Lett. **48** (1982) 322.

[32] K. C. Shaing, S. A. Hokin, Phys. Fluids **28** (1983) 2136.

[33] J. R. Cary, S. G. Shasharina, Phys. Rev. Lett. **78** (1997) 674.

[34] H. Weitzner, Phys. Plasmas **4** (1997) 575.

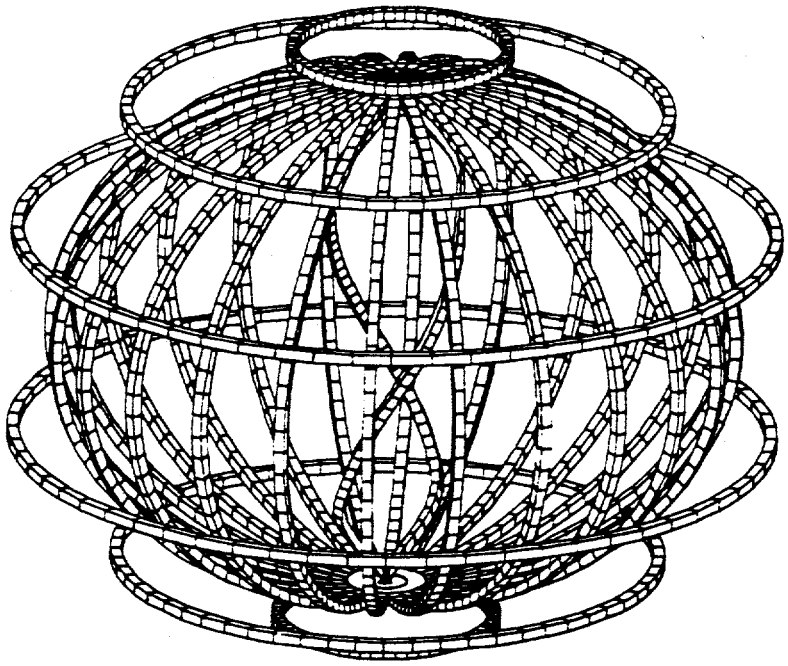

Fig. 1. The coil system of the DHS.

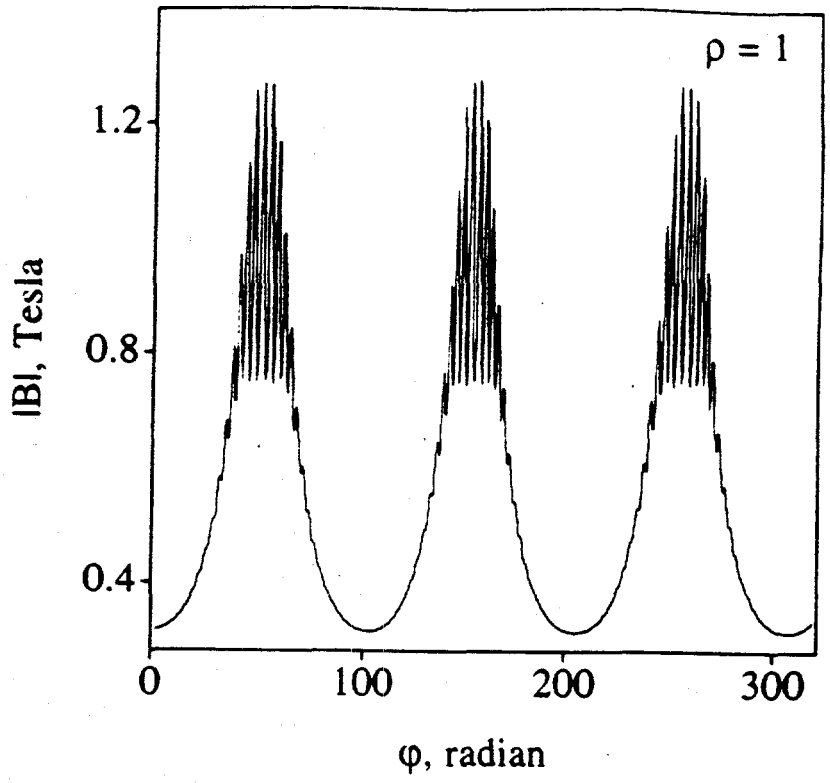

Fig. 2. |B| variation along a field line for the last closed vacuum flux surface.

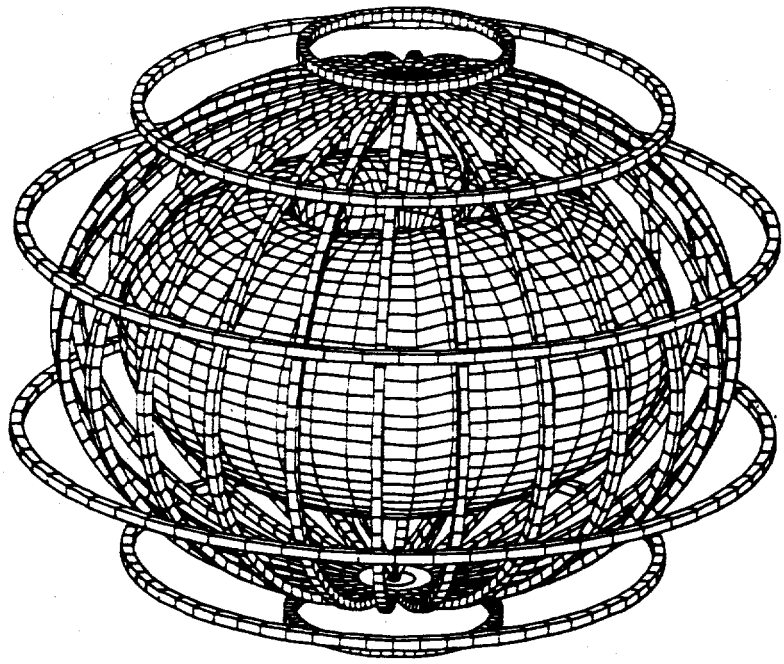

Fig. 3. Perspective view of the last closed vacuum flux surface and the coils of the DHS.

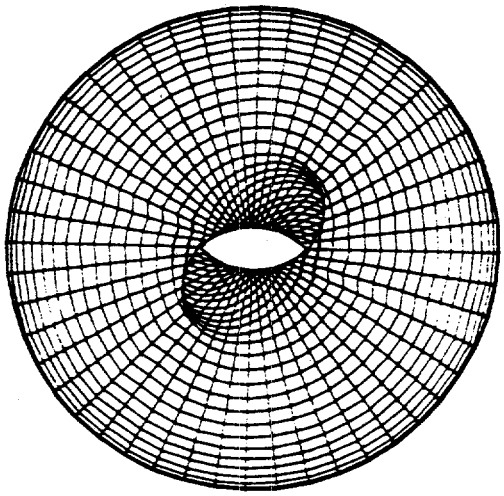

Fig. 4. Top view on the DHS plasma.

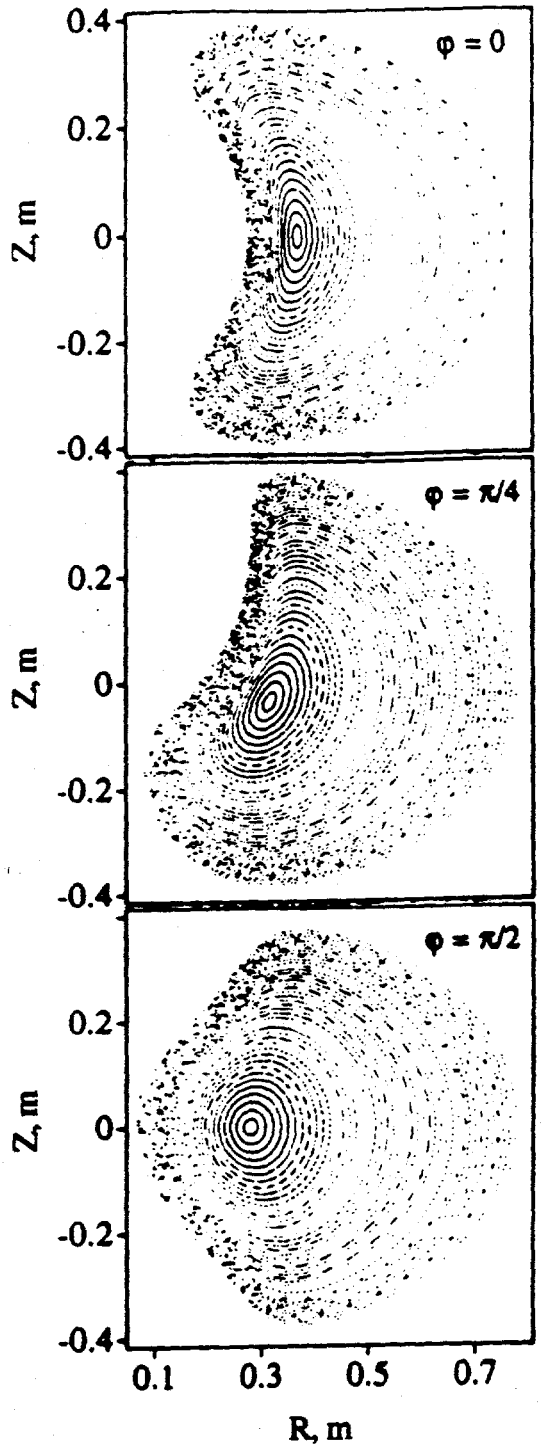

Fig. 5. Poincare puncture plots for closed vacuum flux surfaces in the main cross-sections, $\varphi = 0$, $\pi/4$, and $\pi/2$.

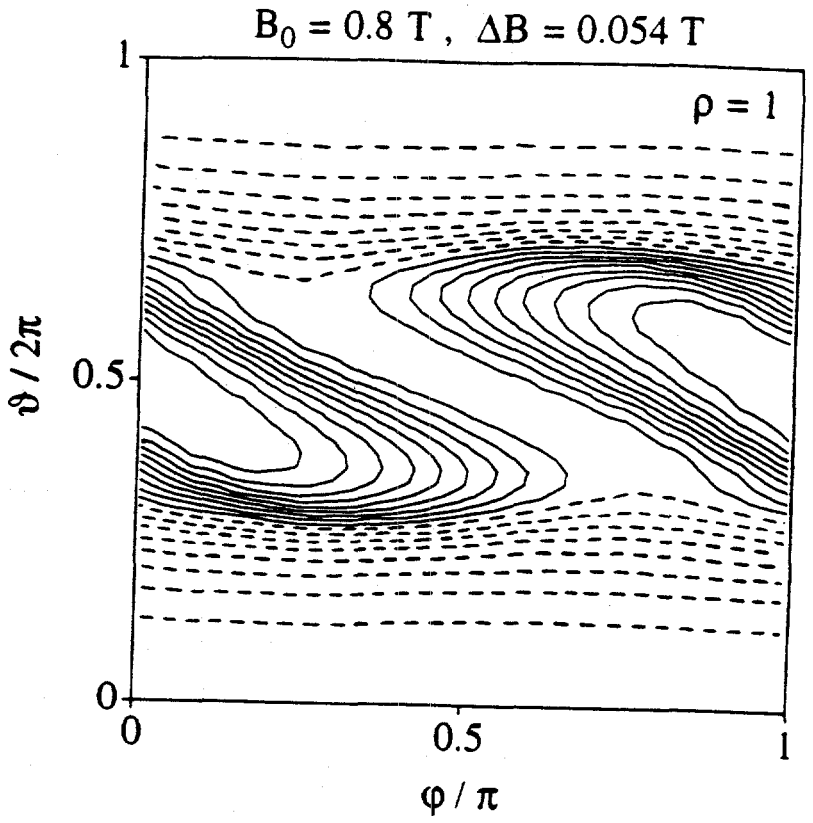

Fig. 6. |B| distribution on the last closed vacuum flux surface. Solid contours are for $B \geq B_0$, dashed - for $B < B_0$, ΔB is the difference between adjacent contours.

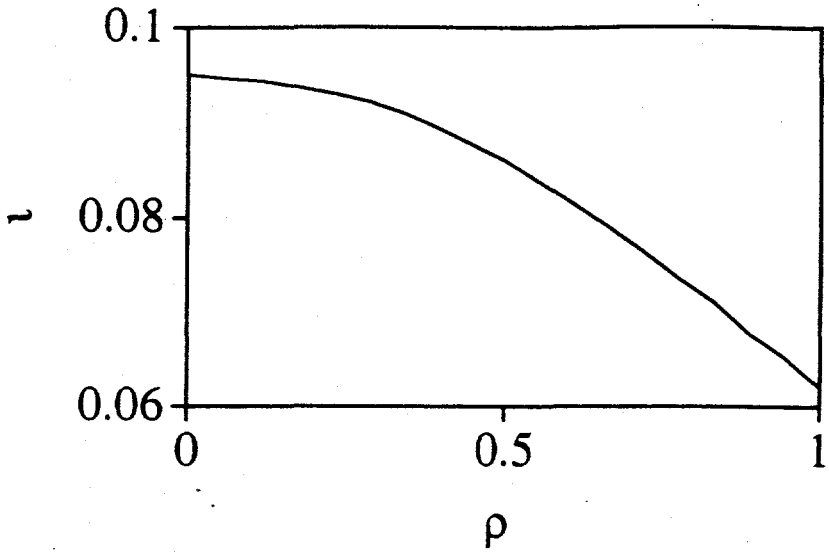

Fig. 7. Vacuum rotational transform.

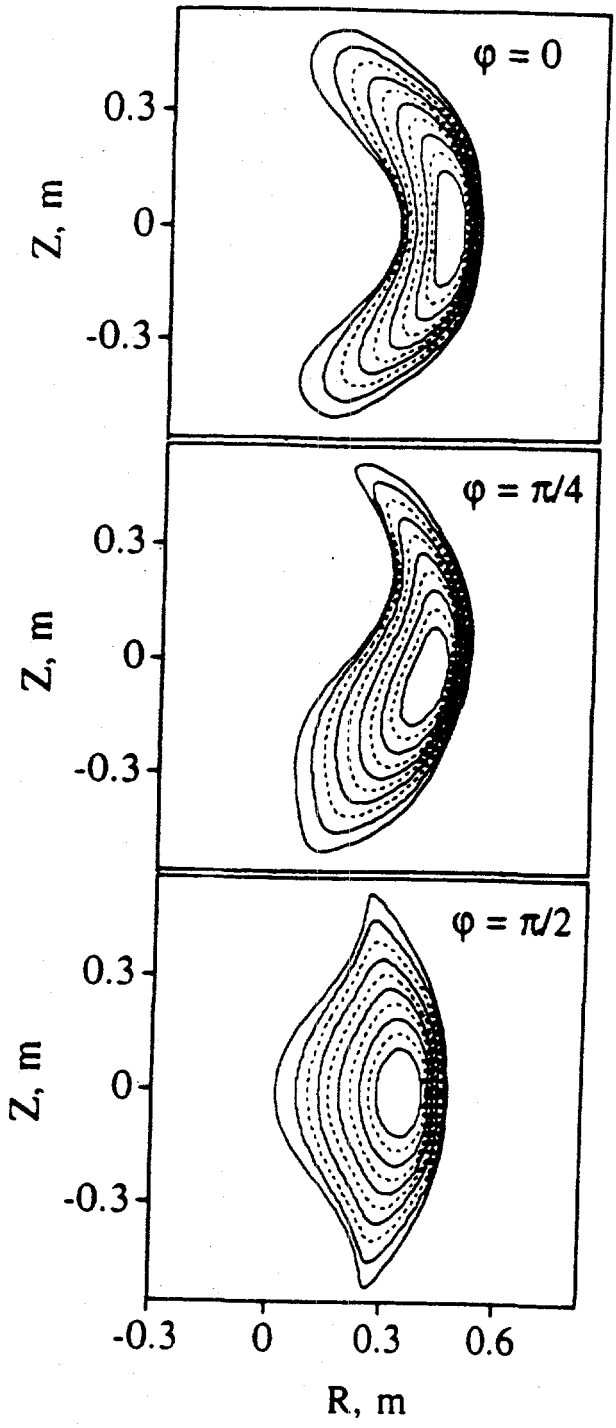

Fig. 8. Three main cross-sections, $\varphi = 0, \pi/4$, and $\pi/2$, for the high-β ($\beta_o = 11\%$, $\beta = 4.5\%$) currentless MHD equilibrium in the DHS.

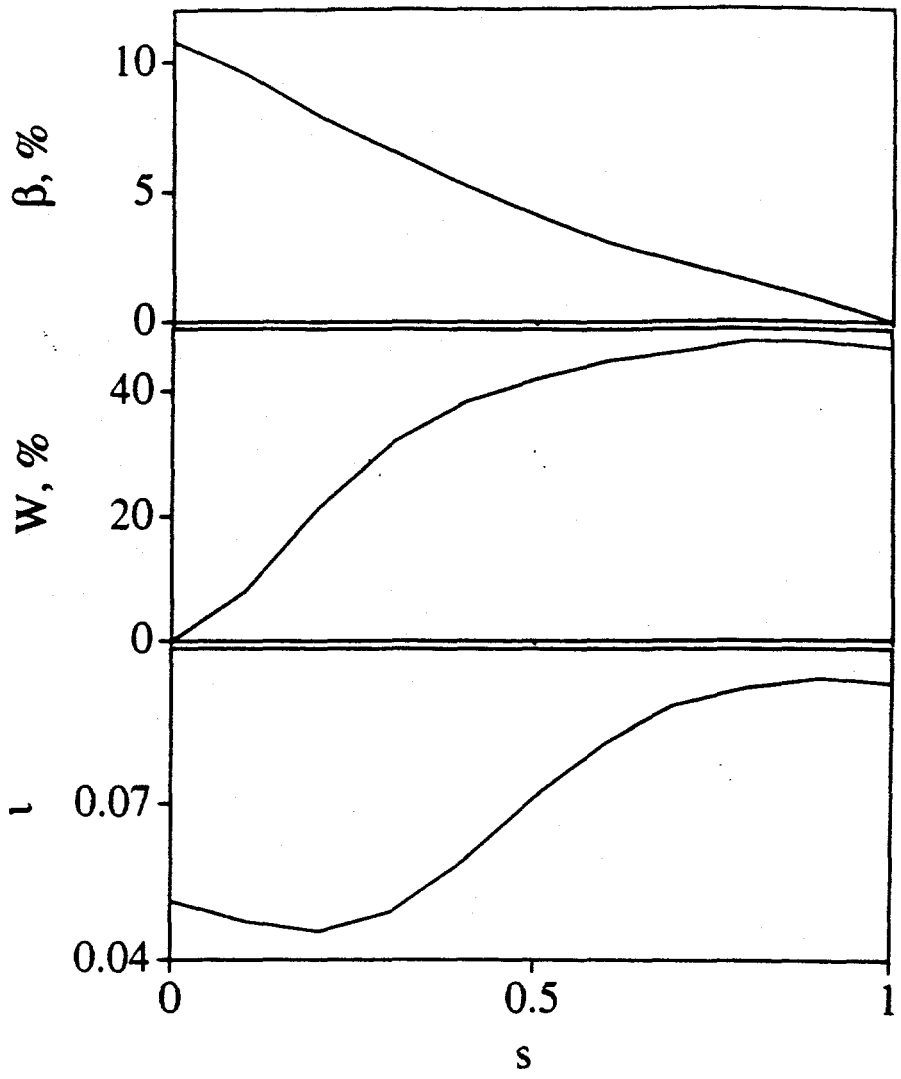

Fig. 9. Radial profiles of β, magnetic well W, and the rotational transform ι for the high-β currentless case of Fig. 8.

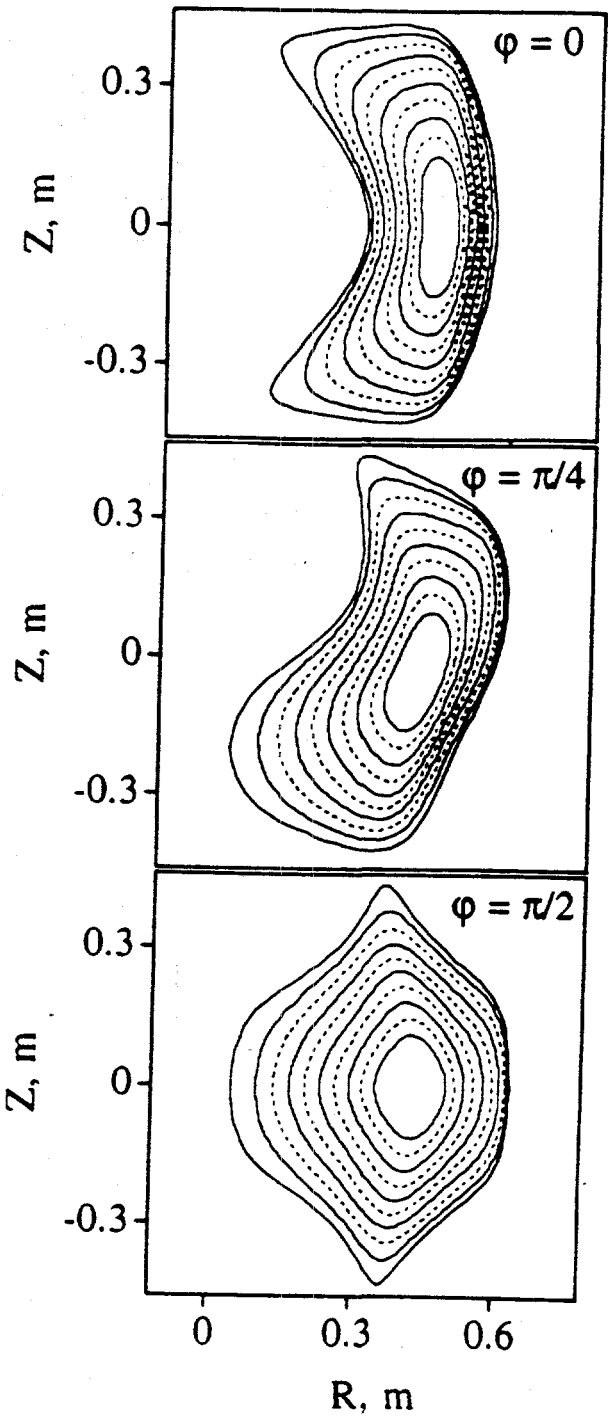

Fig. 10. Three main cross-sections, $\varphi = 0, \pi/4$, and $\pi/2$, for the extreme-high-β ($\beta_o \approx 70\%$, $\beta \approx 30\%$) MHD equilibrium with plasma current of $I_p = 160$ kA.

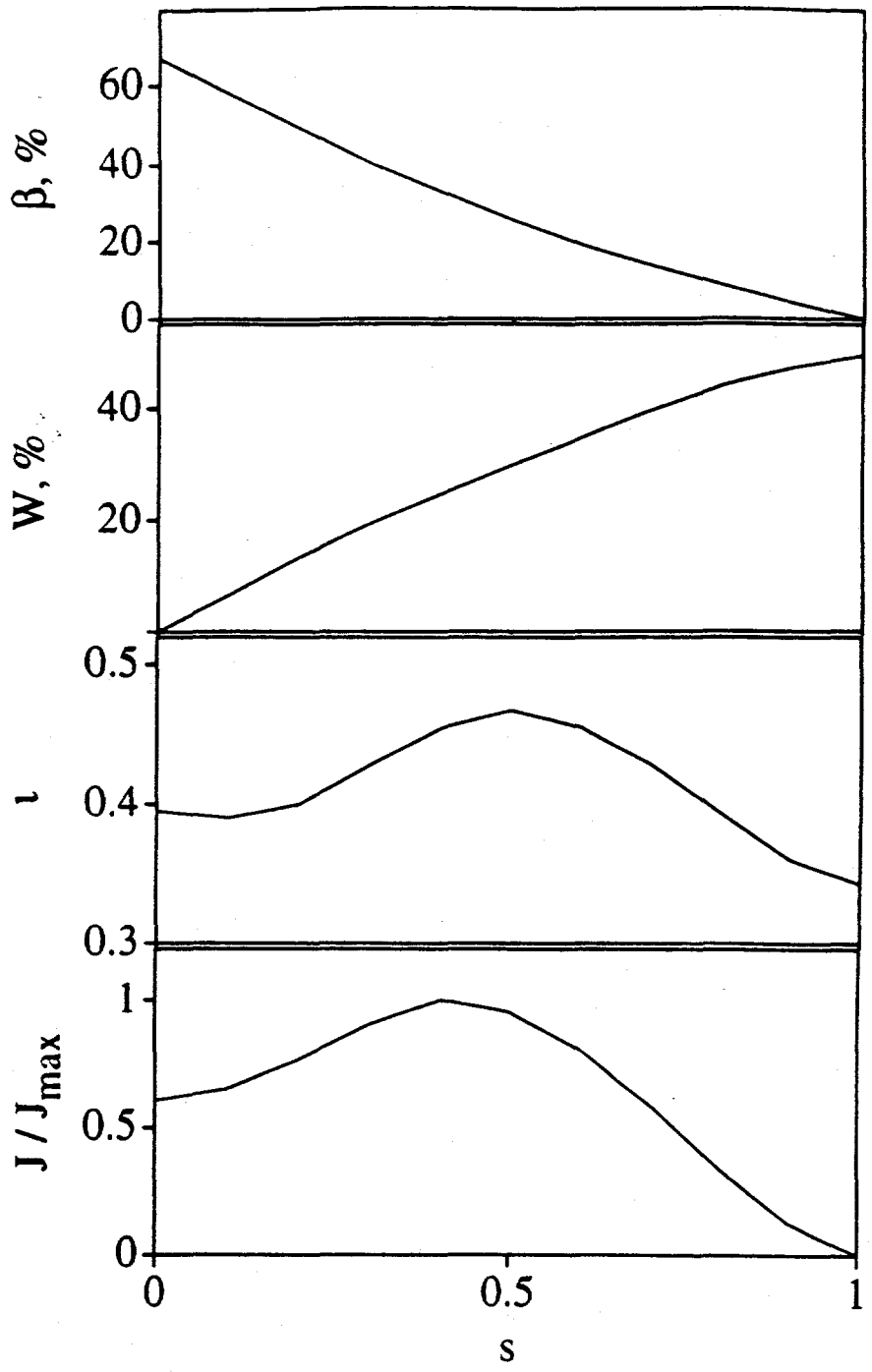

Fig. 11. Radial profiles of β, magnetic well, W, rotational transform, ι, and the normalized plasma current density for the extreme-high-β case of Fig. 10.

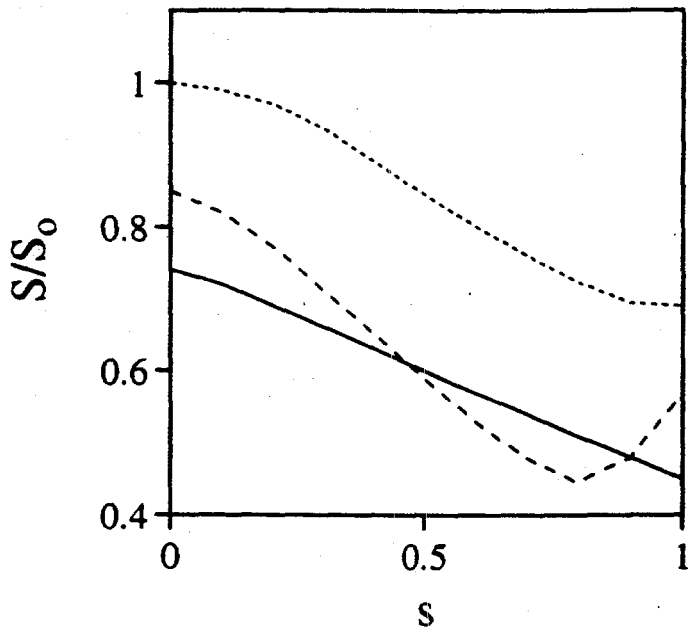

Fig. 12. Radial profiles of S/S_0 for three equilibria considered: vacuum case (solid curve), high-β currentless case (dashed curve), and extreme-high-β equilibrium with the plasma current (dotted curve).